RSC Advances

PAPER

View Article Online
View Journal | View Issue

Cite this: *RSC Adv.*, 2015, **5**, 59403

Ca/Sr ratio dependent structure and up-conversion luminescence of $(Ca_{1-x}Sr_x)In_2O_4 : Yb^{3+}/Ho^{3+}$ phosphors

Ming Guan,[a] Hong Zheng,*[a] Zhaohui Huang,[a] Bin Ma,[a] Maxim S. Molokeev,[bc] Saifang Huang[d] and Lefu Mei*[a]

Received 7th May 2015
Accepted 3rd July 2015

DOI: 10.1039/c5ra08467a

www.rsc.org/advances

Up-conversion (UC) phosphors of $(Ca_{1-x}Sr_x)In_2O_4 : Yb^{3+}/Ho^{3+}$ (x = 0, 0.1, 0.3, 0.5, 0.7, 0.9, 1.0) were prepared. Based on the crystal structure evolution of these series solid solution samples, which were characterized by Rietveld refinement, the variation of UC luminescent properties was discussed in detail. Sr and Ca occupied one position and Yb/Ho dissolved in the In ion site in the $(Ca_{1-x}Sr_x)In_2O_4$ lattice. With increasing Sr substituting Ca atoms, the cell parameters and cell volumes of these samples increased linearly, and distortions of $(Ca/Sr)O_8$ polyhedron were formed. The distortions on crystal structures showed a negative relation with UC luminescent intensities in these series phosphors.

Introduction

The study of up-conversion (UC) phosphors has attracted great attention recently due to its significant potential application in light emitting displays, solid-state lasers, biological labelling, solar energy conversion, and so on.[1,2] As spectral modification materials, UC phosphors showed great importance for converting multiple photons of lower energy into one photon of high energy according to anti-Stokes emission processes. Intense UC luminescence from infrared to visible light was observed widely in many UC phosphors.[3–5]

Recently, some studies showed that the luminescence of ultraviolet excited phosphors always was affected greatly by its crystal structure.[6–10] However, the mechanism of how the crystal structure influences the optical properties of UC materials is still not clear enough. In order to study the relationships between UC luminescence properties and crystal structures, Yb^{3+}/Ho^{3+} co-doped $(Ca_{1-x}Sr_x)In_2O_4$, as well as $CaIn_2O_4$ and $SrIn_2O_4$ were prepared. Indium (In) belongs to the same group with boron, aluminium and gallium, it was suggested as an excellent host lattice for luminescence.[11,12] Recent reports showed that Yb^{3+}/Ho^{3+} co-doped $CaIn_2O_4$ and $SrIn_2O_4$ have excellent UC luminescent properties. $CaIn_2O_4$ and $SrIn_2O_4$ have low phonon energies (~475 cm^{-1}), which is much lower than those of other typical oxide hosts, such as Y_2O_3 (~600 cm^{-1}), silicate (~1100 cm^{-1}), they can therefore achieve high-efficiency UC emissions.[13–17] Previously, the structure of $CaIn_2O_4$ was discussed in literatures, but no correct ICSD (Inorganic Crystal Structure Database) or JCPDS (Joint Committee on Powder Diffraction Standards) file for the $CaIn_2O_4$ is available.[12] In the $SrIn_2O_4$ structure (orthorhombic, *Pnma*, ICSD #16241), two kinds of distorted InO_6 octahedra were connected to form a network, and Sr^{2+} ions located in the middle of the formed pentagonal prism tunnel. As the similarity of Ca^{2+} and Sr^{2+} ions, $(Ca_{1-x}Sr_x)In_2O_4$ shows great potential in the formation of continuous solid solution. As the difference, replacement between Ca and Sr are expected to change the crystal structure slightly and then influence the UC luminescent properties of UC phosphors. For Ho^{3+} and Yb^{3+} ions, they are important activator and sensitizer for UC phosphors, respectively.[18–20]

In this work, UC phosphors of Yb^{3+}/Ho^{3+} co-doped $(Ca_{1-x}Sr_x)In_2O_4$ continuous solid solution were synthesized *via* a solid-state reaction process. According to our previous result, the radio of Yb^{3+}/Ho^{3+} was determined as 0.1/0.005 to get a good UC luminescence.[14] The relationship between crystal structure evolution and UC luminescent properties of this series samples were discussed in detail.

Experimental

Starting materials of $CaCO_3$(A.R.), $SrCO_3$(A.R.), In_2O_3(99.995%), Yb_2O_3(99.995%), Ho_2O_3(99.995%), Yb_2O_3(99.995%) were weighted according to stoichiometric ratio, and then the mixtures were ground thoroughly in an agate mortar. After that, the mixtures were sintered at 1300 °C for 3 hours, with the heating rate of 5 °C min^{-1}, and then cooled to room

[a]*School of Materials Science and Technology, Beijing Key Laboratory of Materials Utilization of Nonmetallic Minerals and Solid Wastes, National Laboratory of Mineral Materials, China University of Geosciences, Beijing 100083, China. E-mail: zhengh@cugb.edu.cn; mlf@cugb.edu.cn*

[b]*Laboratory of Crystal Physics, Kirensky Institute of Physics, SB RAS, Krasnoyarsk 660036, Russia*

[c]*Department of Physics, Far Eastern State Transport University, Khabarovsk 680021, Russia*

[d]*Department of Chemical and Materials Engineering, the University of Auckland, PB 92019, Auckland 1142, New Zealand*

temperature naturally. All the samples were washed for three times by the deionized water and dried for the following measurement.

The X-ray powder diffractometer (D8-ADVANCE, Bruker Corporation, Germany) with Cu-Kα and linear VANTEC detector was used for Rietveld analysis. The step size of 2θ was 0.02°, and the counting time was 2 s per step. Rietveld refinement was performed by using TOPAS 4.2.[21] The UC luminescent spectra were recorded on a spectrophotometer (F-4600, Hitachi, Japan) equipped with an external power-controllable 980 nm semiconductor laser (Beijing Viasho Technology Company, China) as the excitation source. Diffuse reflection spectra were measured on a UV-vis-NIR spectrophotometer (Shimadzu UV-3600, Japan) attached to an integral sphere, and $BaSO_4$ was used as a reference standard. All the measurements were carried out at room temperature.

Results and discussion

X-ray diffraction (XRD) was employed to characterize the structure evolution of all the $0.1Yb^{3+}/0.005Ho^{3+}$ doped $(Ca_{1-x}Sr_x)In_2O_4$ (x = 0, 0.1, 0.3, 0.5, 0.7, 0.9, 1.0) samples. Fig. 1 showed the selected XRD patterns of $(Ca_{0.5}Sr_{0.5})In_2O_4 : Yb^{3+}/Ho^{3+}$ sample, as well as pure $CaIn_2O_4$ and $SrIn_2O_4$. Because of no correct ICSD or JCPDS file for the $CaIn_2O_4$ is available, all X-ray patterns of $(Ca_{1-x}Sr_x)In_2O_4 : Yb^{3+}/Ho^{3+}$ were indexed by orthorhombic cell (*Pnma*) with parameters close to $SrIn_2O_4$ (ICSD #16241), so this crystal structure was used to make Rietveld refinement. In crystal structure there is only one position which can be occupied by Sr and Ca, and this position is multiplied by four positions by symmetry elements (Fig. 2). The occupations of Sr/Ca ions were fixed during refinement. Also Yb^{3+} and Ho^{3+} ions are dissolved in the lattice and substituted In^{3+} ions partly, and their occupancies were fixed. The refinement of all the samples of $(Ca_{1-x}Sr_x)In_2O_4 : Yb^{3+}/Ho^{3+}$, pure $CaIn_2O_4$ and $SrIn_2O_4$ were stable, and ended with low R-factors (shown in Table 1, Fig. 1). $(Ca/Sr)O_8$ square antiprism and

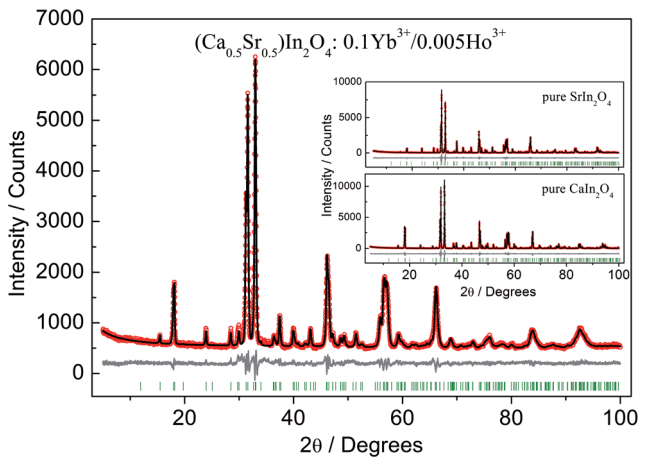

Fig. 1 Observed (red), calculated (black), and difference (gray) XRD patterns for the refinement of $(Ca_{0.5}Sr_{0.5})In_2O_4 : 0.1Yb^{3+}/0.005Ho^{3+}$, as well as pure $CaIn_2O_4$ and $SrIn_2O_4$ samples in the insets.

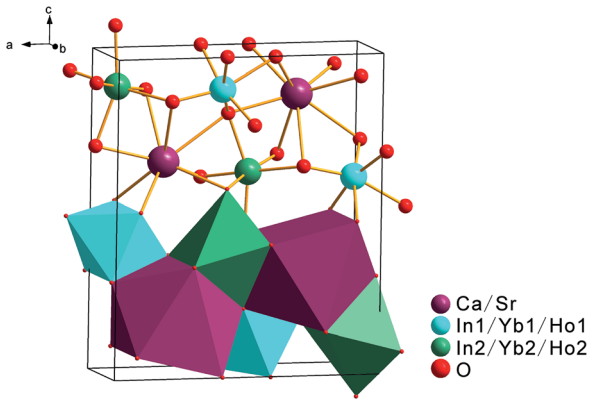

Fig. 2 Crystal structure of the $(Ca_{1-x}Sr_x)In_2O_4 : 0.1Yb^{3+}/0.005Ho^{3+}$ samples.

$(In/Yb/Ho)O_6$ octahedra are existed in the crystal structure simultaneously. The detailed crystal structure of $(Ca_{1-x}Sr_x)In_2O_4 : 0.1Yb^{3+}/0.005Ho^{3+}$ was shown in Fig. 2.

Fig. 3 showed the refined lattice parameters of a, b, c, and unit cell volume (V) as functions of x values in $(Ca_{1-x}Sr_x)In_2O_4 : Yb^{3+}/Ho^{3+}$ (x = 0, 0.1, 0.3, 0.5, 0.7, 0.9, 1.0) samples, and a, b, c, and V value in pure $CaIn_2O_4$ and $SrIn_2O_4$. Since Ca/Sr in eight coordination, and the ionic radii IR (Ca^{2+}, CN = 8) = 1.12 Å, IR (Sr^{2+}, = 1.26 Å),[22] lattice parameters of a, b, c and V of these samples showed a linear increase with the increasing Sr content, indicating that the $(Ca_{1-x}Sr_x)In_2O_4$ formed continuous solid solution. Moreover, pure $CaIn_2O_4$ and $SrIn_2O_4$ have smaller lattice parameters and cell volumes than Yb^{3+}/Ho^{3+} co-doped $CaIn_2O_4$ and $SrIn_2O_4$, respectively. This is because In/Yb/Ho in six coordination, and IR (Yb^{3+}, CN = 6) = 0.868 Å, IR (Ho^{3+}, CN = 6) = 0.901 Å, IR (In^{3+}, CN = 6) = 0.8 Å; Yb^{3+}/Ho^{3+} dopants in $CaIn_2O_4$ or $SrIn_2O_4$ enlarged the unit cells due to their larger IR than In^{3+}, testifying that Yb^{3+} and Ho^{3+} ions occupied the In^{3+} ions sites.

Fig. 4 gave the UC emission spectra of pure $CaIn_2O_4$, $(Ca_{1-x}Sr_x)In_2O_4 : 0.1Yb^{3+}/0.005Ho^{3+}$ (x = 0, 0.1, 0.3, 0.5, 0.7, 0.9, 1.0), and pure $SrIn_2O_4$ upon 980 nm laser excitation. Lacking of rare earth sensitive and active ions, no UC emission was observed in pure $CaIn_2O_4$ and $SrIn_2O_4$ samples. For $(Ca_{1-x}Sr_x)In_2O_4 : Yb^{3+}/Ho^{3+}$, strong green emission with the strongest peak at 546 nm was obtained, which was associated with the characteristic energy level transition of $^5S_2(^5F_4) \rightarrow {}^5I_8$ of Ho^{3+}.[13,17,23] $SrIn_2O_4 : Yb^{3+}/Ho^{3+}$ showed the strongest UC luminescence among all the samples, suggesting that $SrIn_2O_4$ would be an excellent UC host material. Nevertheless, it can be seen that majority of Ca/Sr ratio substituted samples possessed lower UC luminescent intensities than $CaIn_2O_4 : Yb^{3+}/Ho^{3+}$ and $SrIn_2O_4 : Yb^{3+}/Ho^{3+}$ samples.

In order to explain the UC emission intensity differences in Ca/Sr ratio substituted samples, the detailed crystal structures and polyhedrons of some samples were analysed. The $(Ca/Sr)O_8$ polyhedral distortion index, D, can be calculated as followed:

$$D = \frac{1}{n}\sum_{i=1}^{n}\frac{|l_i - l_{av}|}{av}, \quad (1)$$

Table 1 Main parameters of processing and refinement of $(Ca_{1-x}Sr_x)In_2O_4$: $0.1Yb^{3+}/0.005Ho^{3+}$, pure $CaIn_2O_4$ and $SrIn_2O_4$ samples

Compounds	Space Group	*a*, Å	*b*, Å	*c*, Å	*V*, Å^3	R_{wp}%
$CaIn_2O_4$	*Pnma*	9.64847 (10)	3.21443 (3)	11.29593 (11)	350.336 (6)	11.14
$CaIn_2O_4$: $0.1Yb^{3+}$,$0.005Ho^{3+}$	*Pnma*	9.6543(2)	3.21652 (8)	11.3034 (3)	351.007 (15)	12.29
$(Ca_{0.9}Sr_{0.1})In_2O_4$: $0.1Yb^{3+}$,$0.005Ho^{3+}$	*Pnma*	9.6768 (4)	3.22542 (13)	11.3307 (4)	353.65 (2)	11.65
$(Ca_{0.7}Sr_{0.3})In_2O_4$: $0.1Yb^{3+}$,$0.005Ho^{3+}$	*Pnma*	9.7180 (5)	3.24012 (16)	11.3826 (6)	358.41 (3)	9.96
$(Ca_{0.5}Sr_{0.5})In_2O_4$: $0.1Yb^{3+}$,$0.005Ho^{3+}$	*Pnma*	9.7613 (5)	3.25218 (17)	11.4253 (6)	362.70 (3)	10.17
$(Ca_{0.3}Sr_{0.7})In_2O_4$: $0.1Yb^{3+}$,$0.005Ho^{3+}$	*Pnma*	9.7967 (4)	3.25980 (12)	11.4624 (4)	366.06 (2)	9.33
$(Ca_{0.1}Sr_{0.9})In_2O_4$: $0.1Yb^{3+}$,$0.005Ho^{3+}$	*Pnma*	9.8266 (3)	3.26668 (10)	11.4917 (3)	368.886 (19)	11.05
$SrIn_2O_4$: $0.1Yb^{3+}$,$0.005Ho^{3+}$	*Pnma*	9.85194 (17)	3.27340 (6)	11.5178 (2)	371.443 (11)	9.08
$SrIn_2O_4$	*Pnma*	9.83188 (9)	3.26563 (3)	11.49003 (11)	368.914 (6)	10.14

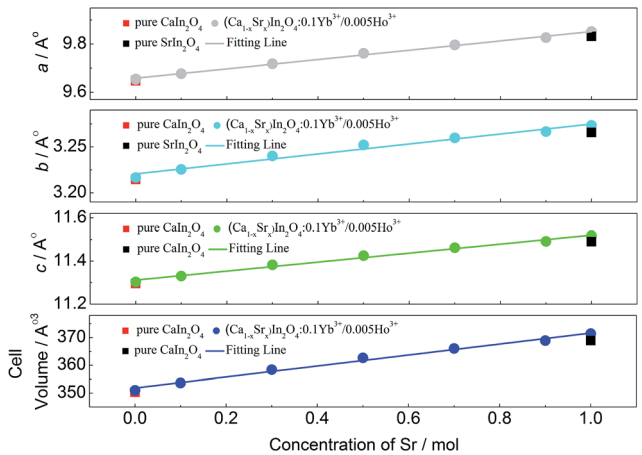

Fig. 3 Refined lattice parameter of *a*, *b*, *c*, and unit cell volume (*V*) showed a linear increase as function of *x* values in $(Ca_{1-x}Sr_x)In_2O_4$: Yb^{3+}/Ho^{3+} ($x = 0$, 0.1, 0.3, 0.5, 0.7, 0.9, 1.0), and *a*, *b*, *c*, *V* values in pure $CaIn_2O_4$ and $SrIn_2O_4$.

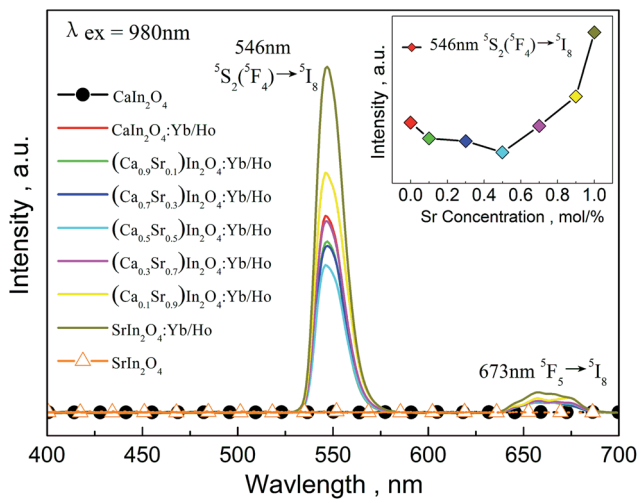

Fig. 4 UC emission spectra of pure $CaIn_2O_4$, $(Ca_{1-x}Sr_x)In_2O_4$: $0.1Yb^{3+}/0.005Ho^{3+}$ ($x = 0$, 0.1, 0.3, 0.5, 0.7, 0.9, 1.0), and pure $SrIn_2O_4$ upon 980 nm laser excitation, and the inset shows the variation of UC emission intensities.

where l_i is the distance between central atom and the i^{th} coordinating atom, and the l_{av} is the mean bond length.[7] The calculated distortion of pure $CaIn_2O_4$, $(Ca_{1-x}Sr_x)In_2O_4$: Yb^{3+}/Ho^{3+} ($x = 0.1$, 0.5, 0.9), and pure $SrIn_2O_4$ were determined as 0.234, 0.267, 0.392, 0.264, 0.223, respectively. With the increased Sr substituting Ca, the UC emission intensities of $(Ca_{1-x}Sr_x)In_2O_4$: Yb^{3+}/Ho^{3+} decreased firstly and then increased, as shown in Fig. 4 and 5(a). Meanwhile, the crystal structures of $(Ca_{1-x}Sr_x)In_2O_4$: Yb^{3+}/Ho^{3+} became distort with the substitution between Ca/Sr, and the distortions enlarged firstly and then reduced, as shown in Fig. 5(b). In Fig. 5(c), the distortions also can be observed from the variations of Ca–O3 bond distances: 2.677 and 2.671 in pure $CaIn_2O_4$, 2.590 and 2.903 in $(Ca_{0.5}Sr_{0.5})In_2O_4$: Yb^{3+}/Ho^{3+}, 2.723 and 2.732 in pure $SrIn_2O_4$.

Fig. 6 gave the diffuse reflection spectra of pure $CaIn_2O_4$, $Ca_{1-x}Sr_xIn_2O_4$: $0.1Yb^{3+}/0.005Ho^{3+}$ ($x = 0.1$, 0.5, 0.9), and pure $SrIn_2O_4$ samples. No absorption bands except for UV region were found in the non-doped $CaIn_2O_4$ and $SrIn_2O_4$. However, absorption valley centred at 449, 540, 643 nm (Ho^{3+} ions) and 980 nm (Yb^{3+} ions) were observed. In Yb^{3+}/Ho^{3+} doped UC phosphors, two channels of excitations are responsible for the impurity luminescence. One is direct excitation of Ho^{3+} ions. The other is indirect excitation, followed by an energy transfer from the Yb^{3+} to the Ho^{3+} ions to cause the luminescence. These

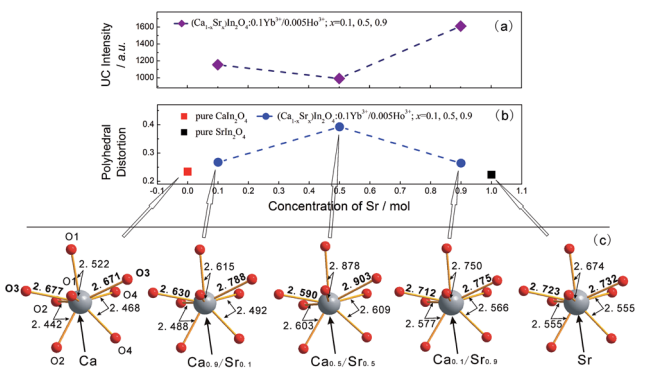

Fig. 5 UC emission intensities at 546 nm of $(Ca_{1-x}Sr_x)In_2O_4$: $0.1Yb^{3+}/0.005Ho^{3+}$ ($x = 0.1$, 0.5, 0.9) (a); calculated distortion indexes of (Ca/Sr)O_8 polyhedron in pure $CaIn_2O_4$, $(Ca_{1-x}Sr_x)In_2O_4$: $0.1Yb^{3+}/0.005Ho^{3+}$ ($x = 0.1$, 0.5, 0.9), and pure $SrIn_2O_4$ (b); (Ca/Sr)O_8 polyhedron of pure $CaIn_2O_4$, $Ca_{1-x}Sr_xIn_2O_4$: $0.1Yb^{3+}/0.005Ho^{3+}$ ($x = 0.1$, 0.5, 0.9), and pure $SrIn_2O_4$ (c).

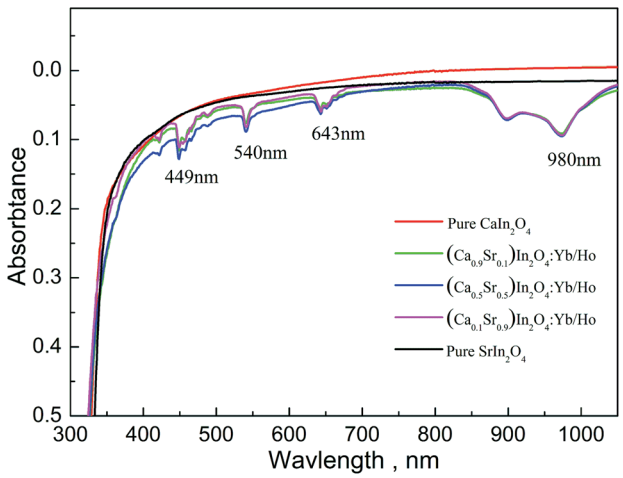

Fig. 6 The diffuse reflection spectra of pure $CaIn_2O_4$, $Ca_{1-x}Sr_xIn_2O_4$: $0.1Yb^{3+}/0.005Ho^{3+}$ (x = 0.1, 0.5, 0.9), and pure $SrIn_2O_4$.

three diffuse reflection patterns of Yb^{3+}/Ho^{3+} co-doped $Ca_{1-x}Sr_xIn_2O_4$ (x = 0.1, 0.5, 0.9) are similar, revealing that the substitution between Ca and Sr did not change the UC luminescence mechanism for Ho^{3+} or Yb^{3+}/Ho^{3+}.

Accordingly, a new model that the distortion (D) of $(Ca/Sr)O_8$ polyhedron has a negative relation with UC luminescent intensity (I) in $(Ca_{1-x}Sr_x)In_2O_4 : Yb^{3+}/Ho^{3+}$ samples was proposed:

$$I \propto \frac{1}{D} \tag{2}$$

The lattice expansion and increased distortion cause by partial substitution for Ca/Sr changed the crystal field acting on the Ho^{3+} or Yb^{3+}/Ho^{3+} ions,[24,25] leading to the variation of UC luminescent properties in the Yb^{3+}/Ho^{3+} co-doped $(Ca_{1-x}Sr_x)In_2O_4$ continuous solid solution phosphors.

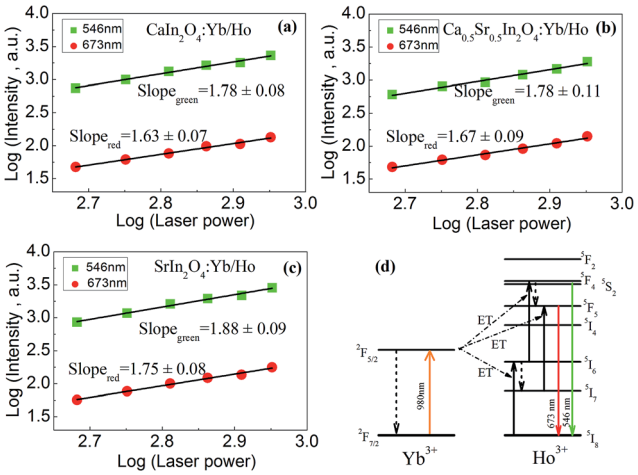

Fig. 7 Dependence of UC emission intensities upon different pumping powers of $CaIn_2O_4 : 0.1Yb^{3+}/0.005Ho^{3+}$ (a), $(Ca_{0.5}Sr_{0.5})In_2O_4 : 0.1Yb^{3+}/0.005Ho^{3+}$ (b), $SrIn_2O_4 : 0.1Yb^{3+}/0.005Ho^{3+}$ (c), and proposed UC luminescence mechanisms in Yb^{3+}/Ho^{3+} doped $(Ca_{1-x}Sr_x)In_2O_4$ phosphors.

Fig. 7 showed the dependence of UC emission intensities upon different pumping powers of $CaIn_2O_4 : Yb^{3+}/Ho^{3+}$(a), typical $(Ca_{0.5}Sr_{0.5})In_2O_4 : Yb^{3+}/Ho^{3+}$(b), and $SrIn_2O_4 : Yb^{3+}/Ho^{3+}$(c). In $(Ca_{0.5}Sr_{0.5})In_2O_4 : Yb^{3+}/Ho^{3+}$ sample, the double logarithmic plot of the integrated intensities of emissions at 546 nm ($^5S_2/^5F_4 \rightarrow {}^5I_8$) and 673 nm ($^5F_5 \rightarrow {}^5I_8$) *versus* the pump powers yields two straight lines with slopes of 1.78 ± 0.11 and 1.67 ± 0.09, respectively. Furthermore, the slopes were determined as 1.78 ± 0.08 and 1.63 ± 0.07 in $CaIn_2O_4 : Yb^{3+}/Ho^{3+}$, as well as 1.88 ± 0.09 and 1.75 ± 0.08 in $SrIn_2O_4 : Yb^{3+}/Ho^{3+}$. These slopes indicated that the UC emissions in all Yb^{3+}/Ho^{3+} co-doped $(Ca_{1-x}Sr_x)In_2O_4$ UC phosphors are two-photon process. Fig. 7(d) proposed the main UC luminescence mechanism of these Yb^{3+}/Ho^{3+} co-doped phosphors. In the present system, the excited Yb^{3+} ions transferred its energy to neighbouring Ho^{3+} ion through energy transfer (ET) process $^2F_{5/2}$ (Yb^{3+}) + $^5I_8$ (Ho^{3+}) → $^2F_{7/2}$ (Yb^{3+}) + $^5I_6$ (Ho^{3+}), $^2F_{5/2}$ (Yb^{3+}) + $^5I_6$ (Ho^{3+}) → $^2F_{7/2}$ (Yb^{3+}) + $^5F_4/^5S_2$ (Ho^{3+}), $^2F_{5/2}$ (Yb^{3+}) + $^5I_7$ (Ho^{3+}) → $^2F_{7/2}$ (Yb^{3+}) + $^7F_5$ (Ho^{3+}), and then the excited Ho^{3+} ion emit green emissions (546 nm, $^5S_2/^5F_4 \rightarrow {}^5I_8$) and red emission (673 nm, $^5F_5 \rightarrow {}^5I_8$).

Conclusions

Ca/Sr ratio dependent structure and up-conversion luminescence of $(Ca_{1-x}Sr_x)In_2O_4 : Yb^{3+}/Ho^{3+}$ (x = 0, 0.1, 0.3, 0.5, 0.7, 0.9, 1.0) phosphors were studied in detail, and the structure evolution of these series samples were showed by Rietveld refinement. With increasing Sr atoms substituting Ca in the $(Ca_{1-x}Sr_x)In_2O_4$ lattice, the cell parameters and cell volumes of these samples increase linearly. Sr^{2+} and Ca^{2+} occupied one position and Yb^{3+}/Ho^{3+} dissolved in the In^{3+} site. Since the differences between Sr^{2+} and Ca^{2+}, $(Ca/Sr)O_8$ polyhedron distortions were formed, and these distortions suggested a negative relation with UC luminescent intensities in these series phosphors. The UC luminescent properties, pumping powers study and possible UC mechanism of these samples also were discussed.

Acknowledgements

This present work was supported by the National Natural Science Foundations of China (Grant no. 51202226), the Fundamental Research Funds for the Central Universities (Grant no. 2652014125, 2652013128, 2652013043), and the Research Fund for the Doctoral Program of Higher Education of China (Grant no. 20130022110006).

Notes and references

1 R. Martín-Rodríguez, S. Fischer, A. Ivaturi, B. Froehlich, K. W. Krämer, J. C. Goldschmidt, B. S. Richards and A. Meijerink, *Chem. Mater.*, 2013, **25**, 1912.
2 F. Wang and X. Liu, *Chem. Soc. Rev.*, 2009, **38**, 976.
3 Z. G. Xia, P. Du and L. B. Liao, *Phys. Status Solidi A*, 2013, **210**, 1734.

4 A. I. Orlova, S. N. Pleskova, N. V. Malanina, A. N. Shushunov, E. N. Gorshkova, E. E. Pudovkina and O. N. Gorshkov, *Inorg. Mater.*, 2013, **49**, 696.
5 Z. Xia, J. Li, Y. Luo, L. Liao and J. Varela, *J. Am. Ceram. Soc.*, 2012, **95**, 3229.
6 X. Yu, Y. Qin, M. Gao, L. Duan, Z. Jiang, L. Gou, P. Zhao and Z. Li, *J. Lumin.*, 2014, **153**, 1.
7 K. A. Denault, J. Brgoch, M. W. Gaultois, A. Mikhailovsky, R. Petry, H. Winkler, S. P. DenBaars and R. Seshadri, *Chem. Mater.*, 2014, **26**, 2275.
8 F. Cheng, Z. Xia, X. Jing and Z. Wang, *Phys. Chem. Chem. Phys.*, 2015, **17**, 3689.
9 H. Ji, Z. Huang, Z. Xia, M. S. Molokeev, X. Jiang, Z. Lin and V. V. Atuchin, *Dalton Trans.*, 2015, **44**, 7679.
10 H. Ji, Z. Huang, Z. Xia, M. S. Molokeev, V. V. Atuchin, M. Fang and S. Huang, *Inorg. Chem.*, 2014, **53**, 5129.
11 A. Baszczuk, M. Jasiorski, M. Nyk, J. Hanuza, M. Mączka and W. Stręk, *J. Alloys Compd.*, 2005, **394**, 88.
12 J. W. Tang, Z. G. Zou and J. H. Ye, *Chem. Mater.*, 2004, **16**, 1644.
13 T. Li, C. Guo, Y. Yang, L. Li and N. Zhang, *Acta Mater.*, 2013, **61**, 7481.
14 M. Guan, H. Zheng, L. Mei, Z. Huang, T. Yang, M. Fang and Y. Liu, *Infrared Phys. Technol.*, 2014, **67**, 107.
15 T. Li, C. Guo and L. Li, *Opt. Express*, 2013, **21**, 18281.
16 M. Guan, H. Zheng, L. Mei, M. S. Molokeev, J. Xie, T. Yang, X. Wu, S. Huang and Z. Huang, *J. Am. Ceram. Soc.*, 2015, **98**, 1182.
17 F. Kang, X. Yang, M. Peng, L. Wondraczek, Z. Ma and J. Qiu, *J. Phys. Chem. C*, 2014, **118**, 7515.
18 X. Li, J. Zhu, Z. Man, Y. Ao and H. Chen, *Sci. Rep.*, 2014, **4**, 4446.
19 R. Martín-Rodríguez and A. Meijerink, *J. Lumin.*, 2014, **147**, 147.
20 M. Peng and L. Wondraczek, *J. Am. Ceram. Soc.*, 2010, **93**, 1437.
21 Bruker AXS, *TOPAS V4 – User's Manual*, Bruker AXS, Karlsruhe, Germany, 2008.
22 R. D. Shannon, *Acta Crystallogr., Sect. A: Cryst. Phys., Diffr., Theor. Gen. Crystallogr.*, 1976, **32**, 751.
23 S. Zhou, S. Jiang, X. Wei, Y. Chen, C. Duan and M. Yin, *J. Alloys Compd.*, 2014, **588**, 654.
24 M. Peng, N. Zhang, L. Wondraczek, J. Qiu, Z. Yang and Q. Zhang, *Opt. Express*, 2011, **19**, 20799.
25 R. Xie, N. Hirosaki, M. Mitomo, Y. Yamamoto and T. Suehiro, *J. Phys. Chem. B*, 2004, **108**, 12027.